



Neutron spectroscopy of nickel deuteride



V.E. Antonov^{a,*}, A.S. Ivanov^b, M.A. Kuzovnikov^a, M. Tkacz^c

^aInstitute of Solid State Physics RAS, 142432 Chernogolovka, Moscow District, Russia

^bInstitut Laue Langevin, 6, rue Jules Horowitz, BP 156, F-38042 Grenoble, France

^cInstitute of Physical Chemistry PAS, Kasprzaka 44/52, 01-224 Warsaw, Poland

ARTICLE INFO

Article history:

Available online 18 March 2013

Keywords:

Metal hydrides
Inelastic neutron scattering
Phase equilibria

ABSTRACT

A powder sample of *fcc* NiD synthesized under a deuterium pressure of 0.9 GPa at room temperature is studied at ambient pressure and 10 K by inelastic neutron scattering in the range of energy transfers 22–356 meV. The fundamental band of optical deuterium vibrations in NiD consists of a peak at 62 meV with a shoulder toward higher energies. The second and third optical bands demonstrate approximately harmonic behavior. The spectrum of NiD is similar to that of NiH compressed along the energy scale by a factor of $r = 1.43(2) \approx \sqrt{2}$ characteristic of vibrations of D and H atoms in the same harmonic potential. Thermodynamic calculations using this value of $r = 1.43$ for optical vibrations in NiH and NiD accurately reproduce the experimental difference between the decomposition pressures of NiH and NiD near room temperature.

© 2013 Elsevier B.V. All rights reserved.

1. Introduction

Nickel hydride belongs to a rather large family of hydrides of the group VI–VIII transition metals, in which hydrogen atoms occupy octahedral interstitial positions in the close-packed metal lattices with a *fcc*, *hcp*, or *double hcp* structure [1]. An occupancy of all octahedral positions gives an atomic ratio of H/Me = 1. The spectra of optical hydrogen vibrations in the monohydrides synthesized so far (*fcc* and *hcp* CrH, *hcp* MnH, *dhcp* FeH, *fcc* CoH, *fcc* NiH, *hcp* MoH, *fcc* RhH and *fcc* PdH) have earlier been studied by inelastic neutron scattering (see [2,3] and references therein). Irrespective of the type of the metal lattice, the first band of optical H vibrations in each of these hydrides consists of a strong peak with a broad shoulder extending toward higher energies. In all hydrides except for RhH [3], the second and the third optical H bands appear at energies approximately two and three times the energy of the first band, which is characteristic of harmonic vibrations.

The effect of H substitution by D has earlier been investigated by inelastic neutron scattering (INS) for one of these monohydrides, PdH [4], and also for non-stoichiometric PdH_{0.63} [5]. The optical spectra of the deuterides proved to be very similar to the spectra of the hydrides compressed along the energy scale by factors of $r = 1.51(2)$ and $1.49(2)$, respectively. These values considerably differ from $\sqrt{m_H/m_D} \approx \sqrt{2} \approx 1.41$ for the H and D atoms vibrating in the same harmonic potential well. The factor $r \approx 1.5$ indicates that the force constants for H atoms in PdH are by $\approx 13\%$ larger than those for D atoms in PdD.

In the present paper, we studied the spectrum of optical vibrations in *fcc* NiD in order to examine if $r > \sqrt{2}$ is typical of hydrides and deuterides of other group VI–VIII transition metals. A comparison of this spectrum with the spectrum of *fcc* NiH measured earlier [6] gave a nearly “harmonic” value of $r = 1.43(2) \approx \sqrt{2}$ despite the fact that the Ni–H/D system is a close analog of the Pd–H/D system in many other respects. We also calculated the difference between the decomposition (equilibrium) pressures of NiH and NiD. The calculation using $r = 1.43$ well reproduced the experimental dependence of this difference in a rather wide temperature interval of ± 100 °C around room temperature. Using $r = 1.51$ characteristic of the Pd–H/D system resulted in the dependence inconsistent with experiment.

2. Experimental details

A 3 g batch of powdered nickel metal of 99.5 wt.% purity and a grain size of 3–7 μm was loaded with deuterium in a D₂ gas of 99.995 wt.% purity compressed to 0.9 GPa at room temperature using the high-pressure apparatus described in [7]. In view of the sluggish kinetics of the NiD formation under these conditions [8], the sample was first activated by exposing it to the high deuterium pressure for 24 h followed by degassing under ambient conditions for 30 min. In the second run, the sample was exposed to the 0.9 GPa deuterium pressure for another 24 h, cooled to –50 °C, decompressed and further stored in liquid nitrogen to prevent deuterium losses. An X-ray diffraction study of the obtained sample at ambient pressure and $T = 85$ K showed it to consist of 47 wt% of unreacted *fcc* Ni with the lattice parameter $a = 3.517(3)$ Å and 53 wt% of *fcc* NiD with $a = 3.724(4)$ Å.

The INS spectrum from the powder Ni–D sample was measured at 10 K in the range of energy transfers, E , from 22 to 356 meV with an energy resolution of $\delta E/E \approx 5$ –8% using the IN1-BeF neutron spectrometer installed at the hot source of the high-flux reactor at the Institut Laue-Langevin in Grenoble. The E value was calculated by subtracting 3.5 meV, the mean energy of neutrons that passed through the cold Be filter, from the energy of the incoming neutrons selected with

* Corresponding author. Tel.: +7 496 522 4027.

E-mail address: antonov@issp.ac.ru (V.E. Antonov).

a focusing Cu(220) single crystal. The background spectrum from the cryostat and an empty flat sample holder made of thin aluminum foil was measured separately and then subtracted from the raw INS spectrum of the sample.

3. Results and discussion

3.1. Inelastic neutron scattering

The obtained INS spectrum $S(Q, E)$ of the NiD sample is shown in Fig. 1 together with the spectrum of NiH, which was measured earlier with the same neutron spectrometer IN1-Bef [6]. As one can see, the spectrum of optical vibrations in NiD is very similar to the NiH spectrum compressed along the energy scale. The first fundamental band of optical vibrations in NiD consists of a strong peak at $E = 62$ meV broadened toward higher energies. The second and the third optical bands resulting from multiphonon neutron scattering have a smoother intensity distribution and appear at energies approximately two and three times the energy of the fundamental band, respectively.

The scattering intensity below 38 meV mostly results from the acoustic vibrations in NiD and also in the unreacted Ni remained in the sample. The acoustic spectra of NiH and, for comparison, of Ni were earlier measured by INS at energies down to 2 meV [9]. The acoustic spectrum of NiD should be very similar to that of NiH because the scaling factor E_H/E_D for acoustic vibrations, which equals to $\sqrt{(m_{Ni} + m_D)/(m_{Ni} + m_H)} = 1.008$ in the harmonic approximation, is close to unity due to the large mass $m_{Ni} = 58.71$ a.u. of the Ni atom compared to the masses $m_H = 1.008$ a.u. and $m_D = 2.014$ a.u. of the atoms of hydrogen isotopes.

In the case of optical vibrations, the neutron scattering intensity is proportional to the neutron scattering cross-section σ of the vibrating atom and inversely proportional to its mass m . As a result, the optical part of the INS spectrum from NiD well represents the density of states of the D vibrations, because the contribution from the Ni atoms does not exceed 5%. At the same time, a small impurity of less than 0.1 at.% H in NiD produces a parasitic feature of noticeable intensity – a peak of the H local modes – at energies of 86–106 meV (see Fig. 1) due to the anomalously large $\sigma_H \approx 10.7\sigma_D$ [10] and $m_H \approx m_D/2$.

As one can see, e.g., from Fig. 2b, the shape of the high-energy shoulder of the fundamental optical peak in NiD differs from that

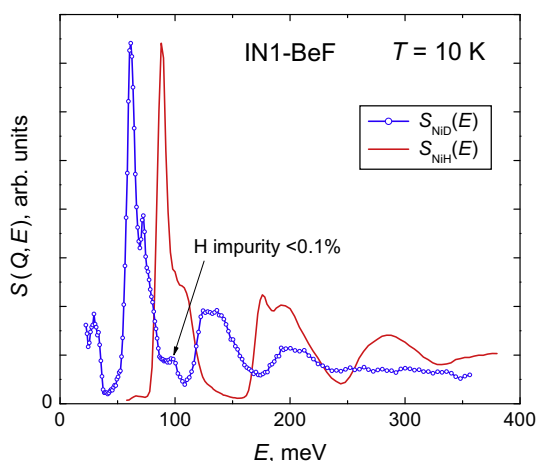


Fig. 1. The dynamical structure factors $S(Q, E)$ of fcc NiD (open circles, present work, $T = 10$ K) and fcc NiH (thin solid curve [6], $T = 5$ K) as functions of the energy loss E of the inelastically scattered neutrons. The depicted spectrum of NiH [6] was measured for an angle $\psi = 45^\circ$ between the vector Q of neutron momentum transfer and the [100] axis of the (001)[100] texture of the bulk planar sample; this orientation made the spectrum virtually indistinguishable from the powder spectrum.

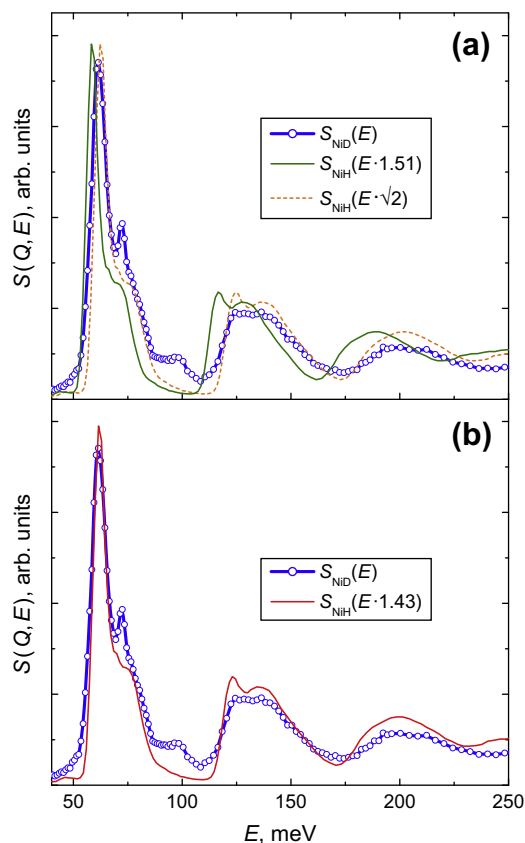


Fig. 2. Comparison of the experimental INS spectrum of NiD (open circles) and the spectrum of NiH [6] compressed along the energy scale using the scaling factors $r = 1.51$ and $\sqrt{2}$ (a) and the factor $r = 1.43$ (b).

in NiH. The origin of this difference is not clear at the moment. In the case of NiD, the additional scattering intensity could result (at least, partly) from the band of covibrations of the H and D atoms. Such a band located at energies right above the main optical peak was recently observed in hydrogen-doped Pd samples [4].

As seen from Fig. 2a, the positions of the second and third optical bands in NiD are well represented by the INS spectrum of NiH compressed along the energy scale by a ‘harmonic’ factor $r = \sqrt{2}$. As shown in Fig. 2b, using a little larger factor of $r = 1.43$ additionally helps to better reproduce the position of the fundamental optical peak at 62 meV. Thus, in contrast to the Pd–H/D system, the force constants for D in the deuteride and for H in the hydride in the Ni–H/D system do not differ within the experimental accuracy.

The density $g_{NiH}(E)$ of optical phonon states in NiH presented in Fig. 3 is derived from the experimental $S(Q, E)$ spectrum of NiH measured in [6] and shown in Fig. 1. The method used is briefly described in [11]. Regrettably, this method is inapplicable to the $S(Q, E)$ spectrum of NiD because of its contamination with scattering intensity from the H impurity. The density $g_{NiD}(E)$ of phonon states in NiD is calculated from $g_{NiH}(E)$ assuming that $g_{NiD}(E) = r \cdot g_{NiH}(E \cdot r)$ and using $r = 1.43$.

3.2. Isotope effect in the pressure of phase equilibrium

The T–P phase diagrams shown in Fig. 4 gather together all available experimental data on the pressures of formation (solid symbols) and decomposition (open symbols) of nickel hydride [8,12–17] and deuteride [8,18,19]. The transition pressures determined in our works [14,19] are additionally corrected in accordance with our later, more accurate measurements of the mean

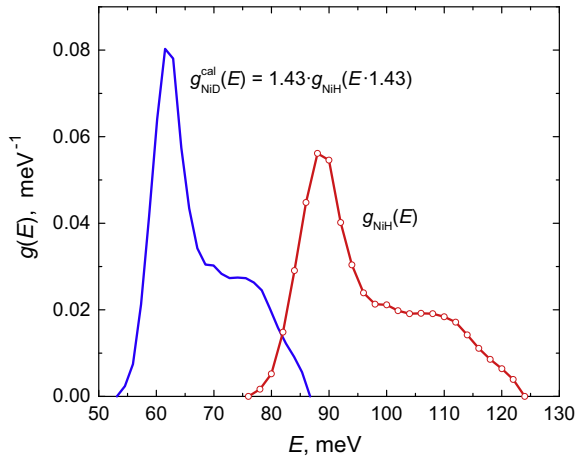


Fig. 3. Densities $g(E)$ of phonon states for optical vibrations in NiH [6] (open circles connected with a solid line) and NiD (solid line) normalized to give $\int g(E)dE = 1$.

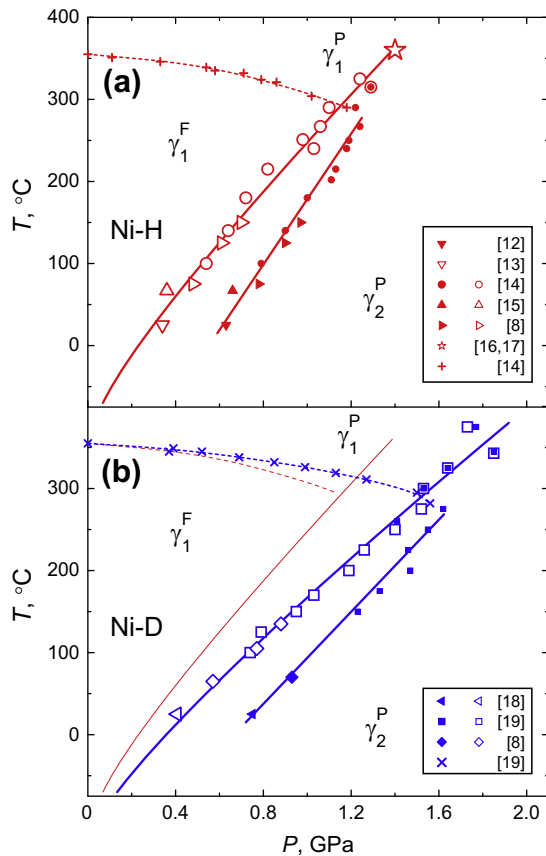


Fig. 4. Experimental T-P phase diagrams of the Ni-H (a) and Ni-D (b) systems. The solid and open symbols show, respectively, the pressures of the $\gamma_1 \rightarrow \gamma_2$ transition (hydride formation) and $\gamma_2 \rightarrow \gamma_1$ transition (hydride decomposition). The open star stands for the critical point of the $\gamma_1 \leftrightarrow \gamma_2$ transformation in the Ni-H system. The crosses indicate the transition temperatures of ferromagnetic γ_1^f solutions to the paramagnetic γ_1^p state (the Curie points). The solid curves representing the $\gamma_2 \rightarrow \gamma_1$ transitions in Fig. 4a and b are obtained with the help of Eq. (1) from the straight lines fitted to the experimental $\Delta G^0(T)$ dependences in Fig. 5. The diagram of the Ni-H system is also shown by thin lines in (b) for comparison with the Ni-D diagram.

temperature of the manganine pressure gauge positioned in the zone of strong temperature gradients near the steel obturator of the high-pressure chamber.

At increasing H_2 pressure, fcc nickel hydride (hydrogen-rich solid solution denoted as γ_2 phase in Fig. 4) is formed via an iso-

morphous phase transition from the hydrogen-poor γ_1 solid solution [20]. The equilibrium pressure of the $\gamma_1 \leftrightarrow \gamma_2$ transformation is close to the pressure of the reverse $\gamma_2 \rightarrow \gamma_1$ transition of hydride decomposition (see [21] for discussion and explanation). At room temperature, the $\gamma_2 \rightarrow \gamma_1$ transition is accompanied by an abrupt decrease in the hydrogen solubility from an atomic H/Ni ratio of $x \approx 1$ to $x \leq 0.01$ [20]. The compositions of the coexisting γ_1 and γ_2 phases get closer to each other with increasing temperature, and the line of the $\gamma_1 \leftrightarrow \gamma_2$ equilibrium terminates in a critical point at 360 °C, 1.4 GPa and $x \approx 0.5$ [16,17]. The Curie temperature of the ferromagnetic γ_1 solutions decreases with hydrogen pressure due to the increase in the equilibrium hydrogen solubility [14]. The γ_2 phase is neither ferromagnetic, nor superconducting at temperatures down to 0.3 K [22]. The diagram of the Ni-D system is similar, only the critical point on the line of the $\gamma_1 \leftrightarrow \gamma_2$ transformation is not yet located.

Fig. 5 shows temperature dependences of the standard (at $P_0 = 0.1$ MPa) Gibbs energies of the reactions $Ni + \frac{1}{2}H_2 \rightarrow NiH$ and $Ni + \frac{1}{2}D_2 \rightarrow NiD$ calculated using the equation

$$\Delta G_{NiH}^0(T) = \int_{P_{eq}^H}^{P_0} \Delta V dP = \int_{P_{eq}^H}^{P_0} (V_{NiH} - V_{Ni} - \frac{1}{2}V_{H_2}) dP \approx -\beta_H P_{eq}^H + \frac{1}{2} \int_{P_0}^{P_{eq}^H} V_{H_2} dP \quad (1)$$

for the Ni-H system and a similar equation for the Ni-D system. In this equation, $\beta_H = V_{NiH} - V_{Ni} \approx 1.25 \text{ cm}^3/\text{mol} \approx \beta_D$ [23] is the difference between the molar volumes of NiH and Ni; $V_{H_2}(T, P)$ is the molar volume of hydrogen and $P_{eq}^H(T)$ is the pressure of the $\gamma_1 \leftrightarrow \gamma_2$ equilibrium, which we consider equal to the pressure of the $\gamma_2 \rightarrow \gamma_1$ transition. The molar volumes of H_2 and D_2 were calculated using equations of state from [24] at pressures above 1 MPa and the equation for ideal gases at $0.1 \leq P \leq 1$ MPa.

As seen from Fig. 5, the $\Delta G^0 = \Delta H^0 - T\Delta S^0$ dependences thus obtained are nearly linear in the studied temperature range. Such a linearity is typical of many metal-hydrogen systems (see, e.g., Ref. [25] discussing this phenomenon in the Pd-H system). The solid curves $P_{eq}(T)$ representing the $\gamma_2 \rightarrow \gamma_1$ transitions in Fig. 4a and b are obtained with the help of Eq. (1) from the straight lines $\Delta G_{NiH,fit}^0(T)$ and $\Delta G_{NiD,fit}^0(T)$ fitting the experimental $\Delta G^0(T)$

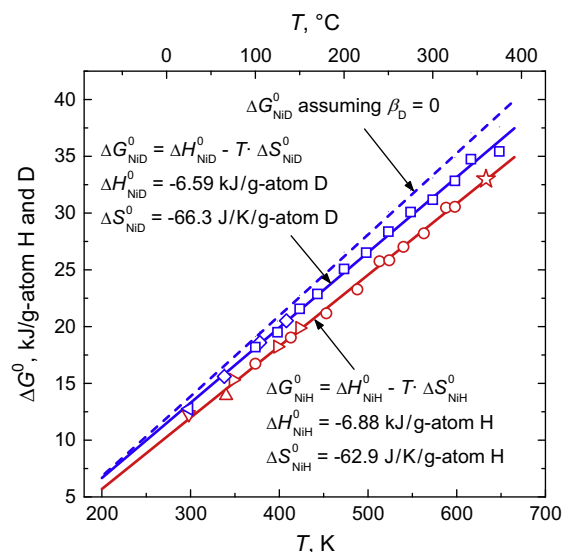


Fig. 5. Temperature dependences of the standard Gibbs energy $\Delta G^0(T)$ for the reactions $Ni + \frac{1}{2}H_2 \rightarrow NiH$ and $Ni + \frac{1}{2}D_2 \rightarrow NiD$ calculated using Eq. (1). The symbols refer to the same experimental points as in Fig. 4.

dependences in Fig. 5 and extrapolated down to -70 °C. We believe this extrapolation is trustworthy.

The invariable values of the standard enthalpy, ΔH^0 , and entropy, ΔS^0 , resulting from the linear fits to the $\Delta G^0(T)$ dependences in Fig. 5 are listed in Table 1. These values and also the values of $\Delta G^0(298\text{ K})$ are slightly different from previous estimates (see [8]) because of the term $-\beta_{\text{H}} P_{\text{eq}}^{\text{H}}$ taken into account in Eq. (1). Neglecting this term in the Ni–D system leads to the $\Delta G^0(T)$ dependence shown in Fig. 5 by the dashed line.

At temperatures below ≈ 100 °C, the hydrogen content of the γ_1 phase is very small and the composition of the γ_2 phase is close to NiH [17,19] therefore the $\Delta G^0(T)$ dependences in Fig. 5 should describe the actual equilibrium in this temperature range. Using the $g_{\text{NiH}}(E)$ and $g_{\text{NiD}}(E)$ spectra allows establishing an interrelation between the lines of the $\text{Ni} + \frac{1}{2}\text{H}_2 \leftrightarrow \text{NiH}$ and $\text{Ni} + \frac{1}{2}\text{D}_2 \leftrightarrow \text{NiD}$ equilibria.

If, e.g., the $\Delta C_{\text{NiD,fit}}^0(T)$ line in Fig. 5 is assumed to represent the equilibrium between Ni and NiD, then the $\Delta C_{\text{NiH}}^0(T)$ line can be calculated. This is because the difference between the free energies of hydride and deuteride of a metal mostly results from the difference in the energies of optical vibrations, which can be written as

$$G_{\text{NiH}}^0 - G_{\text{NiD}}^0 \approx 3N_A kT \int \ln[1 - \exp(-E/kT)] [g_{\text{NiH}}(E) - g_{\text{NiD}}(E)] dE + \frac{3}{2} N_A \int E [g_{\text{NiH}}(E) - g_{\text{NiD}}(E)] dE, \quad (2)$$

where N_A is the Avogadro number, k is the Boltzmann constant and $\int g_{\text{NiH}}(E) dE = \int g_{\text{NiD}}(E) dE = 1$. When this difference is known, the standard formation energy of NiH can be calculated as

$$\Delta C_{\text{NiH,calc}}^0(T) = \Delta C_{\text{NiD,fit}}^0(T) + (G_{\text{NiH}}^0 - G_{\text{NiD}}^0) - \frac{1}{2}(G_{\text{H}_2}^0 - G_{\text{D}_2}^0).$$

The difference $G_{\text{H}_2}^0 - G_{\text{D}_2}^0$ between the Gibbs energies of H_2 and D_2 gases at $P_0 = 0.1$ MPa was calculated in [21] using tabulated data of [26] and proved to vary nearly linearly in a wide temperature interval of 200–1200 K:

$$G_{\text{H}_2}^0 - G_{\text{D}_2}^0 \approx 7.4 + 0.01446 \cdot T \text{ [kJ/mol H}_2 \text{ and D}_2\text{]}.$$

Finally, the calculated values of $\Delta C_{\text{NiH,calc}}^0(T)$ should be substituted in Eq. (1) to be resolved with respect to $P_{\text{eq}}^{\text{H}}(T)$.

If the above procedure is executed with $g_{\text{NiD}}(E) = 1.43 \cdot g_{\text{NiH}}(E - 1.43)$, this gives the $P_{\text{eq}}^{\text{H}}(T)$ dependence shown in Fig. 6 by the thick curve labeled ‘ $r = 1.43$ ’. As one can see, the dependence thus calculated well represents the experimental curve of decomposition of the γ_2 phase in the Ni–H system at temperatures below ~ 150 °C. As is also seen from Fig. 6, the calculated values of $P_{\text{eq}}^{\text{H}}(T)$ are very sensitive to the scaling factor $r = E_{\text{H}}/E_{\text{D}}$, and using $g_{\text{NiD}}(E) = 1.51 \cdot g_{\text{NiH}}(E - 1.51)$ leads to the $P_{\text{eq}}^{\text{H}}(T)$ dependence inconsistent with experiment.

Interestingly, the calculated difference between the decomposition pressures of NiH and NiD appears virtually insensitive to the shape of the $g_{\text{NiH}}(E)$ and $g_{\text{NiD}}(E)$ spectra.

In fact, if we consider the extreme case of the Einstein model with $g^{\text{cg}}(E) = \delta(E - E^{\text{cg}})$ narrowed to a δ -function positioned at the center of gravity, E^{cg} , of the phonon density of states, then Eq. (2) reduces to

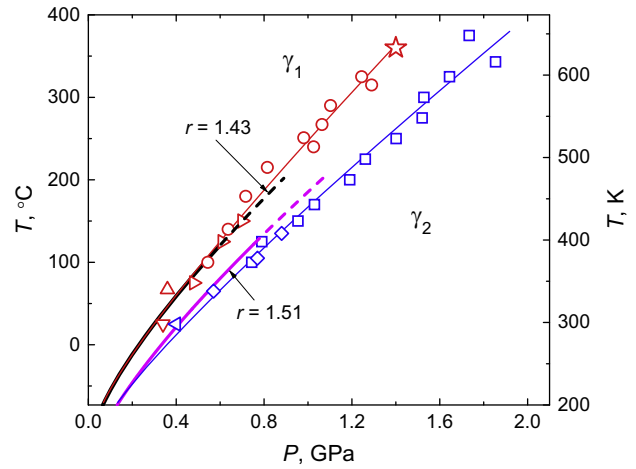


Fig. 6. Temperature dependences of the decomposition pressures of γ_2 phases in the Ni–H and Ni–D systems. The experimental points fitted with the thin solid lines are taken from Fig. 4. The thick curves depict the dependences for the Ni–H system calculated from the experimental dependence for the Ni–D system using scaling factors of $r = 1.43$ and 1.51 (see Section 3.2).

$$G_{\text{NiH}}^0 - G_{\text{NiD}}^0 \approx 3N_A kT \ln[(1 - \exp(-E_{\text{H}}^{\text{cg}}/kT))/(1 - \exp(-E_{\text{D}}^{\text{cg}}/kT))] + \frac{3}{2} N_A (E_{\text{H}}^{\text{cg}} - E_{\text{D}}^{\text{cg}}). \quad (3)$$

Using Eq. (3) with the experimental value of $E_{\text{H}}^{\text{cg}} = 96$ meV and the values of $E_{\text{D}}^{\text{cg}} = E_{\text{H}}^{\text{cg}}/1.43 \approx 67$ meV and $E_{\text{H}}^{\text{cg}}/1.51 \approx 64$ meV gives temperature dependences of the NiH decomposition pressures coinciding within the line thickness with those calculated using Eq. (2) (thick lines in Fig. 6).

4. Conclusions

An INS study of NiD has shown that the D atoms in NiD vibrate in virtually the same, approximately harmonic potential as the H atoms in NiH. A similar conclusion also follows from comparing the experimental and calculated differences in the decomposition pressures of NiD and NiH. This is a rather unexpected result because the Ni–H/D system is the closest analog of the Pd–H/D system and the force constants responsible for optical vibrations in PdH are significantly stronger than in PdD. Moreover, hydrides of some other *d*-metals of the VI–VIII groups are likely to have stronger force constants than the deuterides.

In particular, a higher value of superconducting temperature for the compound with a heavier hydrogen isotope (the reverse isotope effect) was observed in *hcp* MoD ($T_c = 1.11$ K) and *hcp* MoH ($T_c = 0.92$ K) [27]. A higher $T_c \approx 11$ K of PdD compared to $T_c \approx 9$ K of PdH is one of the most famous effects attributed to the difference in the force constants for optical vibrations in PdH and PdD [28,29]. By analogy, the reverse isotope effect in the Mo–H/D system could also be ascribed to the stronger force constants in MoH than in MoD.

The reasons why the potential well for the H atoms in PdH is steeper than for the D atoms in PdD are not fully understood yet, and the effect for other metals cannot be predicted theoretically. We believe that inelastic neutron scattering will be most helpful in solving the problem.

Acknowledgements

This work was supported by Grant No. 11-02-00401 from the Russian Foundation for Basic Research and by the Program ‘‘The Matter under High Energy Density’’ of the Russian Academy of Sciences.

Table 1

Standard enthalpy ΔH^0 , entropy ΔS^0 and Gibbs energy $\Delta G^0(298\text{ K})$ of formation of NiH and NiD resulting from linear fits to the $\Delta G^0(T)$ dependences in Fig. 5.

System	ΔH^0 (kJ/mol Ni)	ΔS^0 (J/K/mol Ni)	$\Delta G^0(298\text{ K})$ (kJ/mol Ni)
Ni–H	-6.9 ± 0.3	-62.9 ± 0.5	11.8 ± 0.3
Ni–D	-6.6 ± 0.5	-66.3 ± 1.0	13.2 ± 0.5

References

- [1] V.E. Antonov, Phase transformations, crystal and magnetic structures of high-pressure hydrides of *d*-metals, *J. Alloys Comp.* 330–332 (2002) 110–116.
- [2] V.E. Antonov, K. Cornell, B. Dorner, V.K. Fedotov, G. Grosse, A.I. Kolesnikov, F.E. Wagner, H. Wipf, Neutron spectroscopy of γ manganese hydride, *Solid State Commun.* 113 (2000) 569–572.
- [3] V.E. Antonov, T.E. Antonova, V.K. Fedotov, B.A. Gnesin, A.S. Ivanov, A.I. Kolesnikov, Anharmonicity of optical hydrogen vibrations in RhH, *J. Alloys Comp.* 446–447 (2007) 508–511.
- [4] V.E. Antonov, A.I. Davydov, V.K. Fedotov, A.S. Ivanov, A.I. Kolesnikov, M.A. Kuzovnikov, Neutron spectroscopy of H impurities in PdD: covibrations of the H and D atoms, *Phys. Rev. B* 80 (2009) 134302–1–134302–7.
- [5] J.J. Rush, J.M. Rowe, D. Richter, Direct determination of the anharmonic vibrational potential for H in Pd, *Z. Phys. B: Condens. Matter* 55 (1984) 283–286.
- [6] V.E. Antonov, V.K. Fedotov, B.A. Gnesin, G. Grosse, A.S. Ivanov, A.I. Kolesnikov, F.E. Wagner, Anisotropy in the inelastic neutron scattering from *fcc* NiH, *Europhys. Lett.* 51 (2000) 140–146.
- [7] B. Baranowski, M. Tkacz, W. Bujnowski, Determination of absorption-desorption isotherms in metal–hydrogen system in the high pressure region, *Roczniki Chem.* 49 (1975) 437–439.
- [8] M. Tkacz, Enthalpies of formation and decomposition of nickel hydride and nickel deuteride derived from (*p*, *c*, *T*) relationships, *J. Chem. Thermodyn.* 33 (2001) 891–897.
- [9] A.I. Kolesnikov, I. Natkaniec, V.E. Antonov, I.T. Belash, V.K. Fedotov, J. Krawczyk, J. Mayer, E.G. Ponyatovsky, Neutron spectroscopy of MnH_{0.86}, NiH_{1.05}, PdH_{0.99} and harmonic behaviour of their optical phonons, *Physica B* 174 (1991) 257–261.
- [10] V.F. Sears, Neutron scattering lengths and cross sections, *Neutron News* 3 (1992) 26–37.
- [11] A.I. Kolesnikov, V.E. Antonov, Yu.E. Markushkin, I. Natkaniec, M.K. Sakharov, Lattice dynamics of AlH₃ and AlD₃ by inelastic neutron scattering: High-energy band of optical bond-stretching vibrations, *Phys. Rev. B* 76 (2007) 064302–1–064302–7.
- [12] T. Skośkiewicz, Investigations of the thermoelectric power at high hydrogen pressure in the Ni–H and Pd–H systems, *Phys. Stat. Sol. (a)* 6 (1971) 29–32.
- [13] B. Baranowski, K. Bocheńska, The decomposition pressure of nickel hydride at 25 °C, *Roczniki Chem.* 36 (1964) 1419–1420.
- [14] E.G. Ponyatovskii, V.E. Antonov, I.T. Belash, T-P phase diagram of the Ni–H system at temperatures to 630°K and pressures to 18 kbar, *Dokl. Akad. Nauk SSSR* 229 (1976) 391–393 (in Russian).
- [15] B. Baranowski, Metal-hydrogen systems in the high pressure range, *Z. Phys. Chem. N. F.* 114 (1979) 59–81.
- [16] Y. Shizuku, S. Yamamoto, Y. Fukai, Phase diagram of the Ni–H system at high hydrogen pressures, *J. Alloys Comp.* 336 (2002) 159–162.
- [17] Y. Fukai, S. Yamamoto, S. Harada, M. Kanazawa, The phase diagram of the Ni–H system revisited, *J. Alloys Comp.* 372 (2004) L4–L5.
- [18] A. Stroka, A. Freilich, Formation of nickel deuteride from nickel and gaseous deuterium, *Roczniki Chem.* 44 (1970) 235–237.
- [19] V.E. Antonov, I.T. Belash, E.G. Ponyatovskii, T-P phase diagrams of the Ni–D and Ni–H systems at temperatures to 375 °C and pressures to 20 kbar, *Dokl. Akad. Nauk SSSR* 233 (1977) 1114–1117 (in Russian).
- [20] B. Baranowski, R. Wiśniewski, Formation of nickel hydride from nickel and gaseous hydrogen, *Bull. Acad. Polon. Sci.* 14 (1966) 273–276.
- [21] V.E. Antonov, A.I. Latynin, M. Tkacz, T-P phase diagrams and isotope effects in the Mo–H/D systems, *J. Phys.: Condens. Matter* 16 (2004) 8387–8398.
- [22] V.E. Antonov, I.T. Belash, O.V. Zharikov, A.V. Palnichenko, A study on superconductivities of high pressure phases in the Re–H, Ru–H, Rh–H, and Ni–H systems, *Phys. Stat. Sol. (b)* 142 (1987) K155–K159.
- [23] A. Janko, J. Pielaszek, Lattice spacing determination for the α and β phases of nickel–hydrogen and nickel–deuterium systems, *Bull. Acad. Polon. Sci.* 15 (1967) 569–572.
- [24] M. Tkacz, A. Litwiniuk, Useful equations of state of hydrogen and deuterium, *J. Alloys Comp.* 330–332 (2002) 89–92.
- [25] T.B. Flanagan, J.F. Lynch, Thermodynamics of a gas in equilibrium with two nonstoichiometric condensed phases. Application to metal/hydrogen systems, *J. Phys. Chem.* 79 (1975) 444–448.
- [26] *Thermodynamical Properties of Individual Substances: a Handbook*, Izd. Akad. Nauk SSSR, Moscow, 1962, in Russian.
- [27] V.E. Antonov, I.T. Belash, O.V. Zharikov, A.I. Latynin, A.V. Palnichenko, Superconductivity of molybdenum hydride and deuteride, *Fiz. Tverd. Tela* 30 (1988) 598–600; V.E. Antonov, I.T. Belash, O.V. Zharikov, A.I. Latynin, A.V. Palnichenko, Superconductivity of molybdenum hydride and deuteride, *Engl. Trans. Sov. Phys. Solid State* 30 (1988) 344–345.
- [28] B.N. Ganguly, High frequency local modes, superconductivity and anomalous isotope effect in PdH(D) systems, *Z. Phys.* 265 (1973) 433–439.
- [29] B.N. Ganguly, The Grüneisen constant for the hydrogen mode in the PdH system, *Phys. Lett. A* 46 (1973) 23–24.